Original scientific paper

MECHANICAL CHARACTERIZATION OF ROTATING TRIANGLE SHAPED AUXETIC SKIN GRAFT SIMULANTS

Gurpreet Singh[1], Vivek Gupta[1], Arnab Chanda[1,2]

[1]Centre for Biomedical Engineering, Indian Institute of Technology (IIT) Delhi, India
[2]Department of Biomedical Engineering, All India Institute of Medical Sciences (AIIMS), Delhi, India

Abstract. *The expansion of the skin grafts plays a key role in treating severe burn injuries. Split-thickness skin grafting, which is a well-known technique for stretching donor skin samples beyond its capacity, typically produces expansions which are insufficient to cover large burn areas. In this work, the expansion potential of skin grafts with novel rotating triangle (RT) shaped auxetic incision patterns were investigated extensively. A skin simulant was employed and a range of RT configurations, with internal angles varying from 0° to 135°, were tested through the development of skin graft simulants. Mechanical testing and digital image correlation (DIC) were used to characterize the Poisson's effect, meshing ratios, and induced stresses of the skin graft simulants, up to 50% strains. The 0° model produced the highest negative Poisson's effect and areal expansions. As the internal angle of the auxetic was increased, expansions were observed to decrease significantly. Beyond 60°, positive Poisson's effect and contractions occurred with an increasing trend, and its peak at 105°. At 15° and 120°, the induced strains were observed to be significant, posing risks of skin rupture. Overall, the expansions were observed to be higher at lower strains. Such experimental findings on expansion potentials and estimations of mechanical properties with auxetic skin grafts simulants have not been reported to date, and would be indispensable for further research in skin graft expansion and severe burn injury treatment.*

Key Words: *Skin Graft, Mechanical properties, Simulant, Expansion, DIC, Burns*

1. INTRODUCTION

The skin, which is the first line of body's defense, commonly experience burn injuries, caused due to heat, friction, radiation, and hazardous chemical exposure. Over

180,000 people die every year globally from burn injuries, majorly from low and middle-income countries [1]. Severe burns, if left untreated, may cause hydration, bleeding, and infection. Split thickness skin grafting is a common surgical procedure for treatment of such difficult-to-heal burn injuries. In split thickness skin grating, a small portion of healthy skin is excised from a donor site and projected with a parallel incision pattern using a skin graft mesher [2, 3]. The meshed skin graft is then stretched beyond its capacity over the large burn region and transplanted to cover the damaged skin. The most common skin grafting modality is of the split-thickness type, in which the entire epidermis and some part of dermis are utilized [1, 4]. Previous studies on split-thickness grafts (SGSTs) have indicated significant disparity between their claimed meshing ratio and the real meshing ratio [5-8]. Real meshing ratios as low as 1:1 was reported, which is insufficient for covering severe burn injury sites [1, 2]. Therefore, innovation to produce higher meshing ratios from skin grafts is warranted.

Auxetic structures, commonly known as metamaterials, exhibit negative Poisson's ratio, and are known to offer high expansion potentials. Rotating triangle shaped auxetic structures, in particular, have demonstrated expansion potentials much higher than that offered by traditional skin grafts. Grima et al. [9] modeled rotating triangle structures with varying angles and reported a maximum negative Poisson's ratio of -0.90. Dudek et al. [10] studied the dynamics of the rotating triangle based auxetic patterns and studied the rotating units for understanding the mechanical characteristics through frictional flexible hinges. They observed convergence in incremental Poisson's ratio beyond -1. In addition to the auxetic structure itself, material deformation and shear were found to affect the Poisson's ratio in polymers. To date, there has been no research on the application of such high expansion potential auxetic patterns in skin grafting.

In this work, a range of novel rotating triangle based auxetic variants were tested experimentally on skin simulants in order to understand their expansion potential in skin grafts. Mechanical testing and digital image correlation (DIC) were employed to characterize the biomechanical properties and expansions. The Poisson's ratios, meshing ratios, and induced stresses, were estimated for the skin graft simulants under tensile loading. The findings from this study are anticipated to pave the way for further research in skin graft expansion, for severe burn injury treatment. Section 2 will discuss the modeling, fabrication, and testing of skin graft simulants. Section 3 will present the results and analysis, followed by the conclusions in Section 4.

2. MATERIALS AND METHODS

2.1 Geometrical Modeling of Auxetic Patterns

Skin is a multi-layered tissue consisting of the epidermis (top layer), dermis (intermediate layer), and hypodermis (bottom layer or subcutaneous). The epidermis layer mainly consists of the stratum corneum and is the first line of defense from the outer environment, such as UV radiation, infection, etc. The dermis layer is made of different collagens and elastins with different orientations and provides mechanical strength to the skin [11, 12].The hypodermis layer, i.e., the bottom layer, has heterogeneous material, including the subcutaneous fat covering the muscles [13-15].In this study, the combined mechanical effect of skin's epidermis and dermis were

considered to focus on evaluation of the expansion properties of split-thickness type auxetic skin grafts. SolidWorks 2020 (Dassault Systèmes, France) was used to design the unit cell of the rotating triangle (RT) shaped auxetic structures and the corresponding skin graft models (Fig. 1).
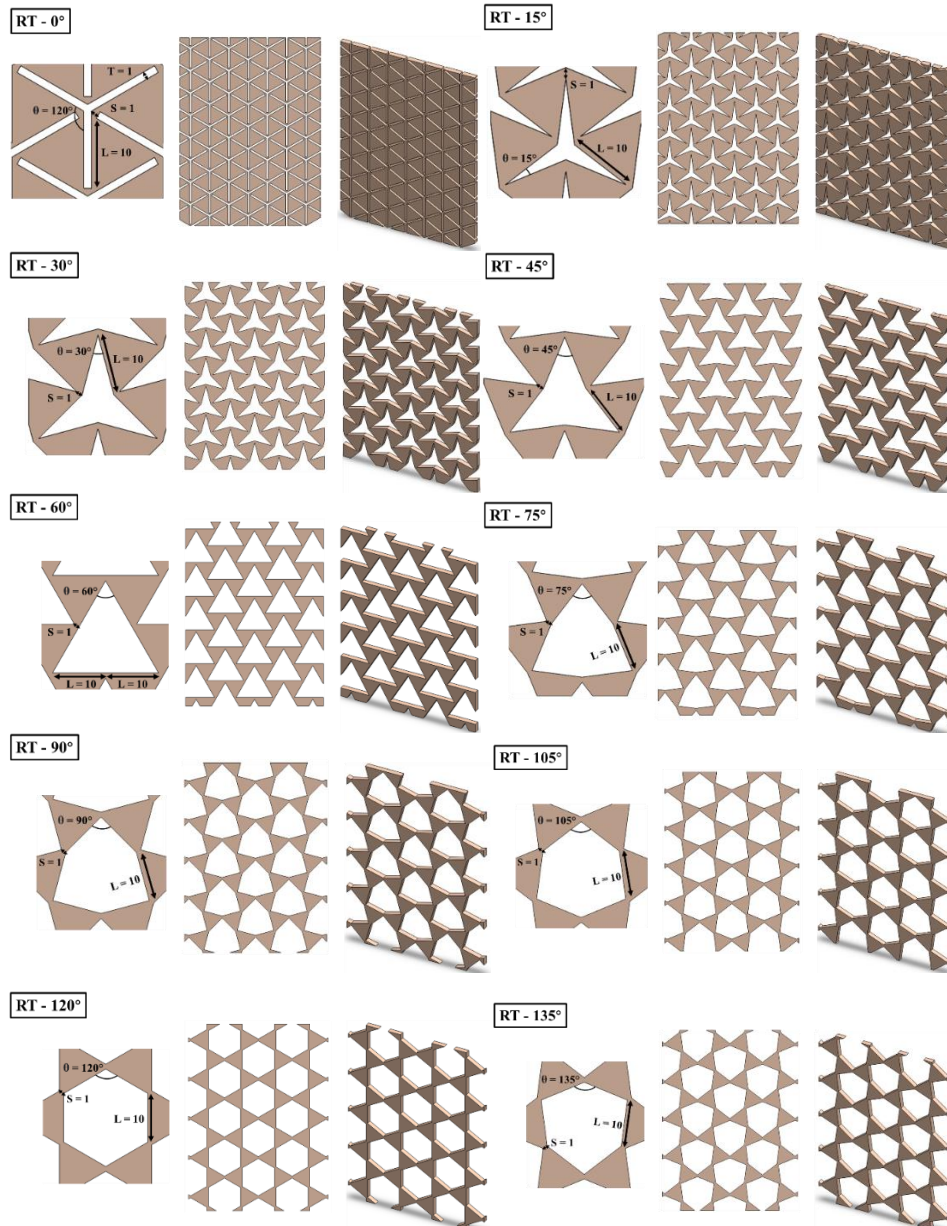

Fig. 1 Unit cell and RT skin graft models with internal angle ranging from 0° to 135°

The dimensions of all the skin graft models were fixed as 100 mm × 75 mm, with a thickness of 2.5 mm. This specific size was chosen to implement symmetric repeating patterns within the skin graft models. The RT angle was varied from 0° to 135° to investigate the changing mechanical properties, effective Poisson's ratio, and induced stresses within the skin graft models. The first pattern of the rotating triangle, RT-0° represented an internal angle of 0°. For the other RT patterns, this angle was varied with an increment of 15º, from 0º to 135º, generating ten skin graft patterns. All these patterns were symmetrically positioned and allowed to run through the edges of the skin model. A unit cell spacing of 1mm for the slits and gaps was considered based on literature studies [1, 16, 17].

2.2 Development of Skin Graft Simulants

The geometrical auxetic models were used to develop negative graft molds with a constant dimension of 100 mm × 75 mm × 2.5 mm (Fig. 2). A Voxelab Aquila 3D printer (Flashforge Technology Ltd, Jinhua, Zhejiang, China) was used to 3D print the STL models of the auxetic graft molds with PLA (Polylactic Acid) material. These 3D printed molds were employed further to cast the skin graft simulants.
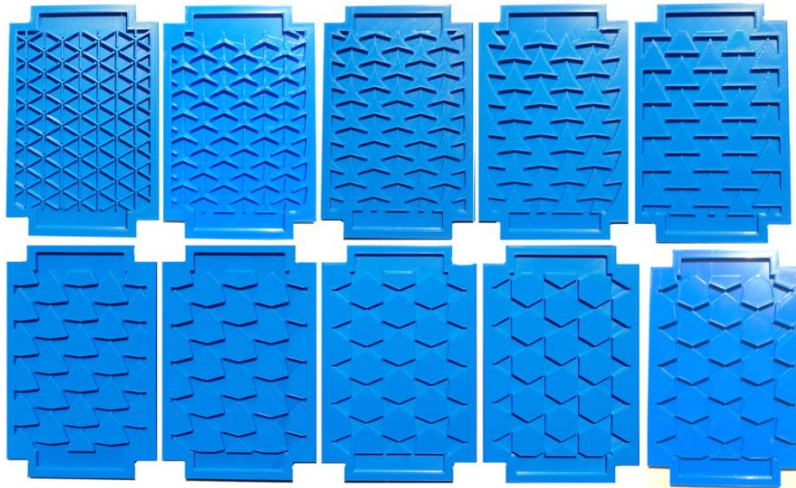

Fig. 2 3D printed skin grafts molds

Multiple skin simulant compositions were developed using silicone, based on previous literature works [1, 16, 18, 19] to fabricate the skin graft simulants. The skin simulant compositions were tested under uniaxial tensile loads at a displacement rate of 0.4 mm/s and compared iteratively with the mechanical properties of the cadaveric human skin [20-24] for determining the most suitable composition for mimicking skin. A two-part silicone material with a shore hardness of 5A was mixed in a 1:1 weight ratio with another two-part silicone material with a shore hardness of 30A. The compositions were thoroughly mixed to obtain shore hardness of 15±2A [11], poured into 3D printed molds (Fig. 2), and left to cure for 8 hours. The hardness of the fabricated skin graft

simulants was measured using shore durometer. The developed skin graft simulants are shown in Fig. 3.
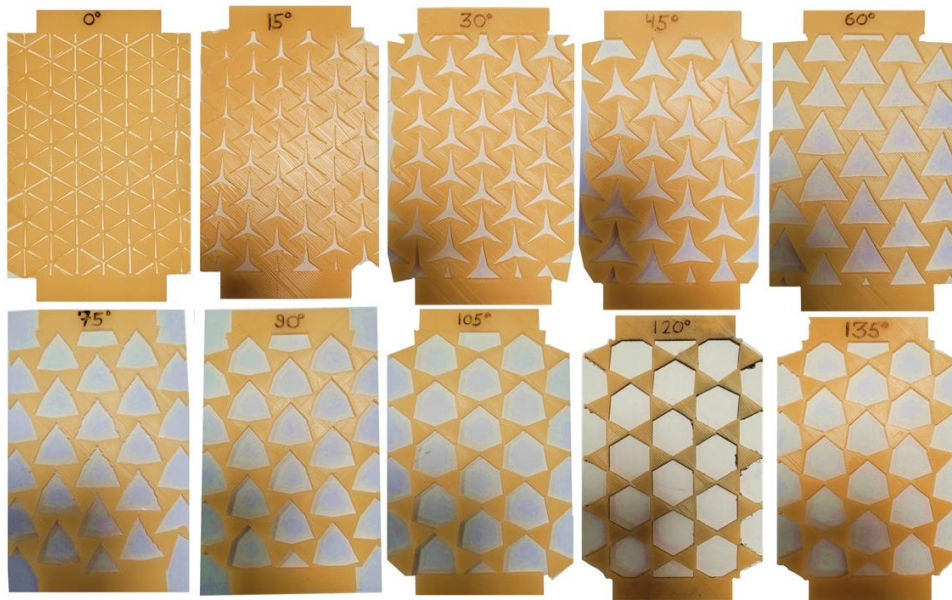

Fig. 3 Skin grafts simulants with varying RT angles

2.3 Mechanical Testing and Digital Image Correlation

The auxetic skin graft simulants were tested at a constant displacement rate of 0.4 mm/s, up to 50% strain. The force-displacement response of the skin graft simulants was measured using a universal testing machine (UTM) (Finetechno Engineering Pvt Ltd, Kolkata, India).The skin graft simulant was clamped on the UTM with one end fixed and as the other end was pulled (see Fig. 4A). The engineering stress-strain plots were generated from the force-displacement data.

On the surface of skin graft simulants, spray paint was used to create dense speckle patterns (Fig. 4B) for the digital image correlation (DIC) analysis. The DIC is a technique to estimate the strain cartographies of a sample during the mechanical testing. In literature, the DIC was used by the researchers to evaluate the strain cartographies of peripherical tissues such as skin [25]. However, to date, strain cartographies have not been estimated for any auxetic structures or grafts, to the best of our knowledge. In this work, the tensile tests were recorded using a high-quality camera (20.1 MegaPixel Sony DSC-W830, Tokyo, Japan) mounted on a tripod stand (Fig. 4C). The distance between a test specimen and the camera was considered on the basis that the camera can record the video of full elongation test (i.e., from start to end). The recorded videos were run through an open-source media player (VideoLAN Client, France) to get 15-20 images for each tensile test. The images were post-processed to calculate the strain fields on the skin graft simulants using VIC-2D software (Correlated Solutions Inc., SC, USA). Based on

the displacement of spray particles, the Lagrangian strain tensor was used for the strain estimation over different deformation phases during tensile testing.
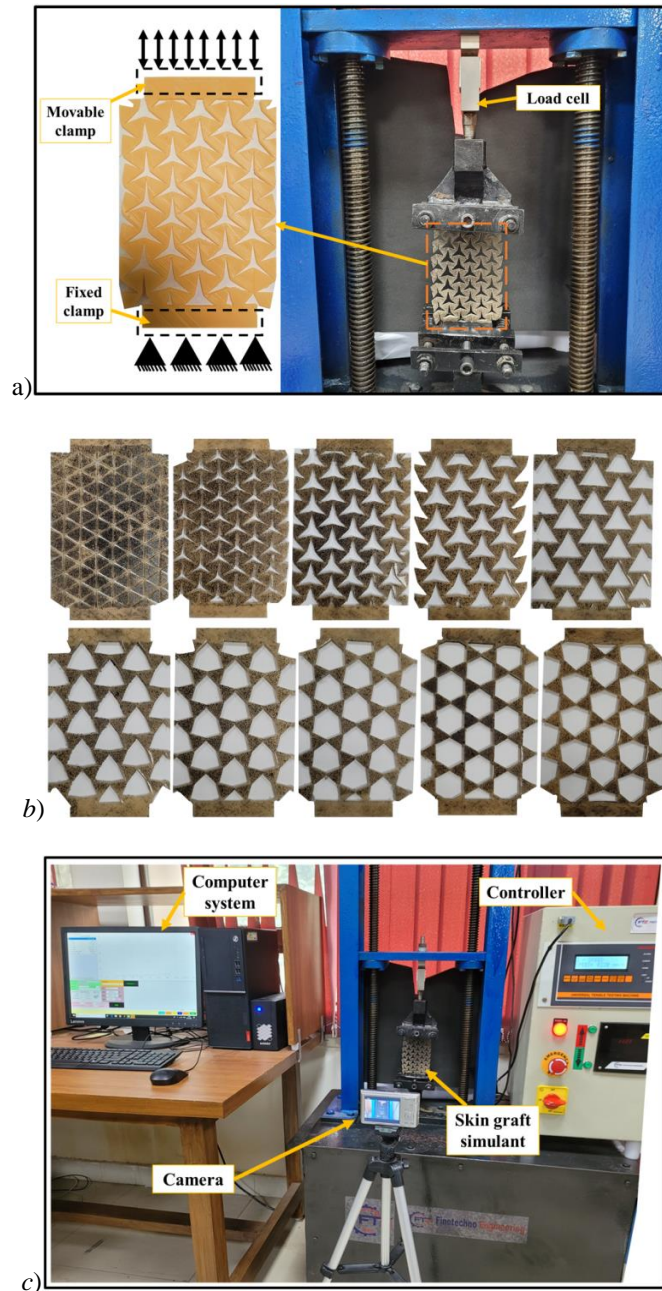

Fig. 4 *a*) Mechanical testing setup for skin graft simulant on the UTM, *b*) densely spray paint speckles, and *c*) DIC setup

3. RESULTS AND DISCUSSION

3.1 Uniaxial Mechanical Properties of Skin Graft Simulants

Across all the skin graft simulants, the stress values were within the range of 0.5 to 19 kPa at 50% strain. The stress versus strain for the skin graft simulants, i.e., RT-0° to RT-135°, is presented in Fig. 5. The maximum stresses were generated in the RT-75° model, and minimum stresses were observed for the RT-0° model. RT-75° and RT-90° exhibited similar stress-strain values after 20% strain and followed the same trend up to 50% strain. Similarly, RT-135°, RT-105°, RT-120°, and RT-60° also showed similar stress-strain behavior. Among all the RT skin graft simulants, RT-0° was determined to be a desirable auxetic structure for skin grafting subjected to the low-stress values. RT-75° and RT-90° skin graft simulants appeared to be the least desirable models.
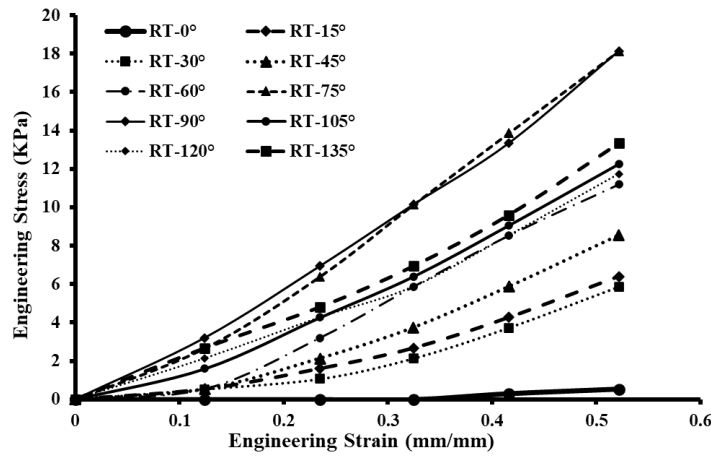

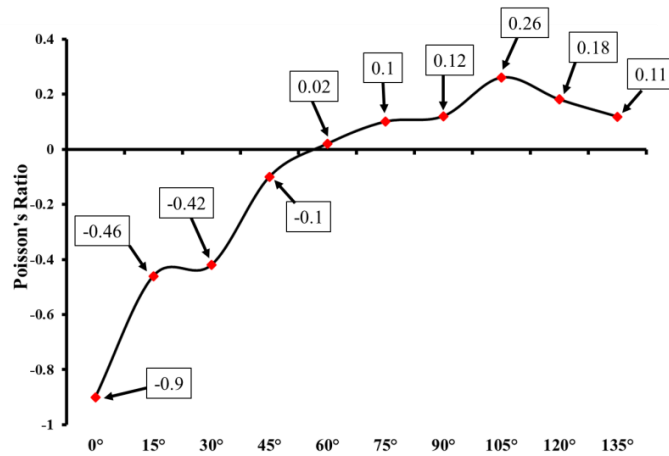**Fig. 5** Stress-strain plot of skin graft simulant models

Fig. 6 Poisson's ratio of RT skin graft simulants at 50% strain

The effective Poisson's ratio was computed in the range of -0.9 to 0.26 for the skin graft simulants with varying angles at 50% strain (Fig. 6). RT-0° skin graft simulant generated the maximum negative Poisson's ratio, while RT-105° showed the minimum Poisson's ratio. Other skin graft simulants exhibited effective Poisson's ratios in between RT-0° and RT-105°. At 50% strain, RT-0°, RT-15°, RT-30° and RT-45° skin graft simulants showed auxetic behavior, and RT-60°, RT-75°, RT-90°, RT-105°, RT-120°, and RT-135° showed non-auxetic behavior. RT-15° and RT-30° skin graft simulants exhibited similar effective Poisson's ratios of -0.46 and -0.42, respectively. It should be mentioned that due to changes in the internal structure of auxetic patterns, the effective Poisson's ratio of skin graft simulants varied with strain [26-28]. For low strain values (RT-0° to RT-45°), the skin graft simulants exhibited auxetic behavior in line with previous findings [29, 30].

3.2 Strain Distribution in Auxetic Skin Graft Models

The skin graft simulants were subjected to stretching up to 50%, and the induced strains were measured using Digital Image Correlation (DIC). At the loading rate of 0.4 mm/s, 50% strain was attained in 125 sec in all models. Significant strain build-up was observed near the UTM clamps across all the skin graft simulants, indicating the possibility of skin rupture (Figs. 7 to 9).
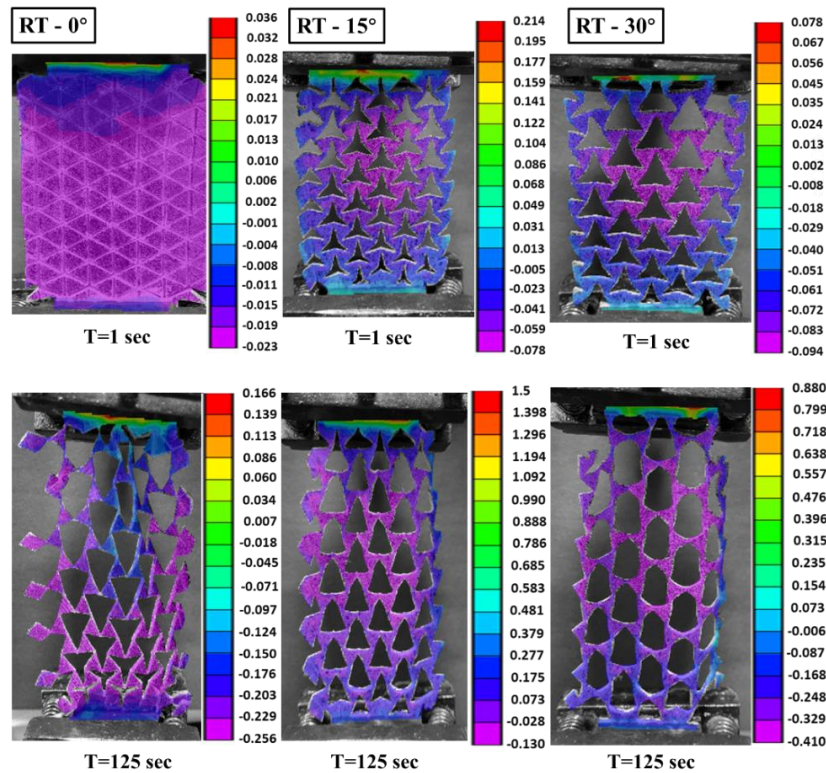

Fig. 7 Strain distribution observed through DIC in skin graft simulants (RT-0° to 30°)
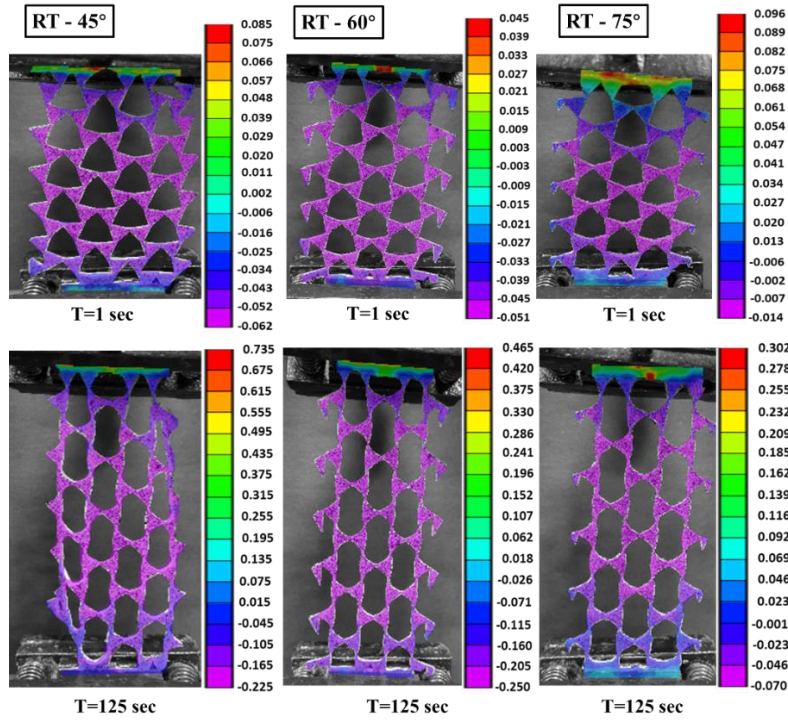
Fig. 8 Strain distribution observed through DIC in skin graft simulants (RT-45° to 75°)
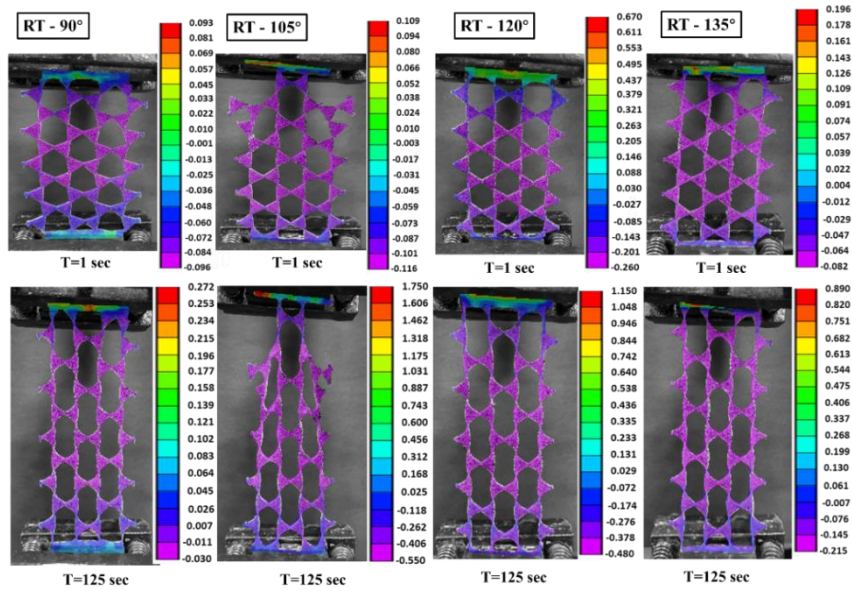

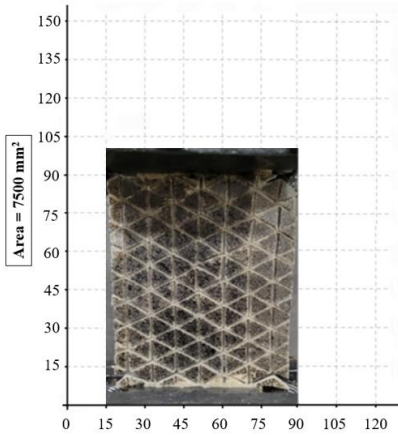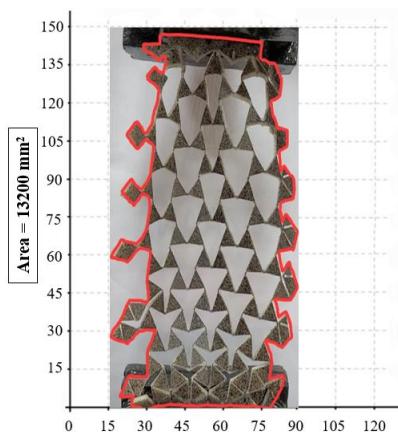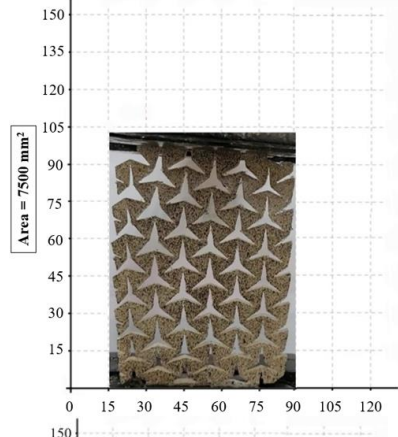**Fig. 9** Strain distribution observed through DIC in skin graft simulants (RT-90° to 135°)
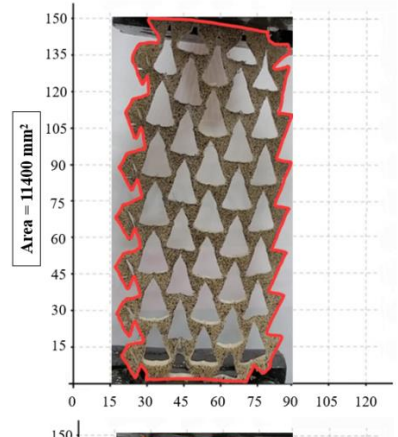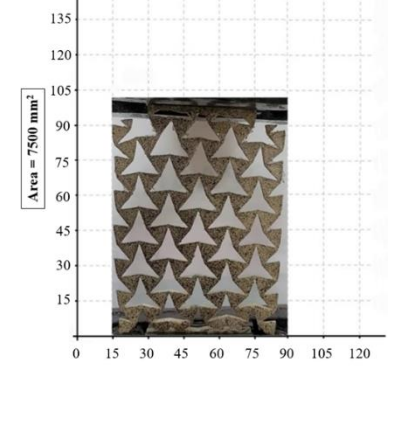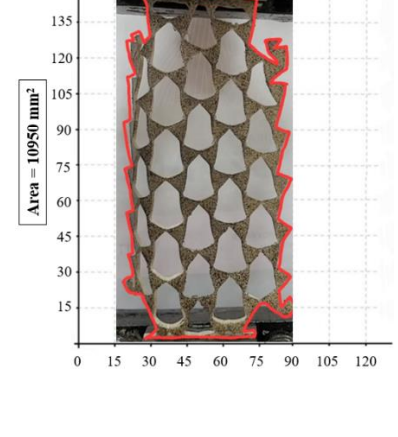
In RT-0° model, the maximum localized strain was very low (i.e., 0.166). A uniform strain distribution was observed across most of the unit cells, except in the upper middle. While RT shaped unit cells were observed closer to the fixed end with uniform stresses all around, triangular unit cells were more prominent at the displacement end, with non-uniform stresses at the edges. The most distorted triangles, transitioning to hexagons, were in the upper middle with wide variation in strains across their edges. In the RT-15° model, several regions exhibited high strain build-ups, including the right edge, top and bottom. The highest strain value recoded was 1.5. All the stretched pattern unit cells were observed to be triangular, with minimal strain build up at the edges. While the high strains at the top and bottom sides could be attributed to the UTM clamping, the strain build up at the right side may be due to the lateral asymmetry and excess skin material presence. In RT-30° model, the maximum strain was almost half (i.e., 0.88) of in the case of RT-15° model. The strain distributions were similar, with all stretched unit cells in shape of hexagon in the case of RT-30° model.

RT-45° showed strain values (i.e., 0.735) lower than RT-30°. The strain distributions were very uniform, unlike in the cases of RT-15° and RT-30°, with fully developed hexagons of nearly similar dimensions. Slight curling at the bottom clamp, and lateral expansion was observed, indicating significant auxetic behavior. In RT-60°, RT-75°, and RT-90° models, fully developed hexagonal unit cells were observed, and the strain distributions were uniform across them. The maximum strains were in the range of 0.272-0.465, much lower than that of RT models with angles of 0° to 45°. The stretched RT-105° model also had fully developed hexagonal unit cells, but a nonuniform strain distribution. The upper half of the model showed higher strain localization compared to the lower half, with a maximum value of 1.41. RT-120° and RT-135° models exhibited similar unit cell shape with uniform strain distributions, with maximum values of 1.15 and 0.89 respectively. RT-135° exhibited similar maximum strain value as that of RT-30°. Due to lower void area in RT-30°, better auxetic properties and expansions are anticipated in RT-30°. Overall, RT-15° model exhibited high possibility of skin rupture at the upper clamp site, followed by RT-105°, and RT-120°. RT-30°, RT-45°, and RT-135° models showed moderate skin rupture possibility. RT-60°, RT-75°, and RT-90° exhibited low possibility of skin rupture, followed by RT-0° which was the least strained model.

### 3.3 Expansion Potential of Skin Graft Simulants

The area estimations of all the skin graft simulants at 0% and 50% strain are shown in Table 1. A constant grid size was used to trace the outer boundaries of the skin graft simulants. The initial area of all the skin graft simulants was 7500 mm^2. The final area of the skin graft simulants varied from 7651 to 13200 mm^2. The maximum area was covered by RT-0° (13200 mm^2) model, and RT-135° (7651 mm^2) showed the minimum covered area. The final area of the other skin graft simulants was: RT-15° (11400 mm^2), RT-30° (10950 mm^2), RT-45° (10350 mm^2), RT-60° (9700 mm^2), RT-75° (8841 mm^2), RT-90° (7914 mm^2), RT-105° (7806 mm^2), RT-120° (7778 mm^2), respectively. The final areas of the skin graft simulants were further used to calculate the meshing ratios and quantify expansion potential.

Table 1 Initial and final area of the skin graft simulants at 50% stretch
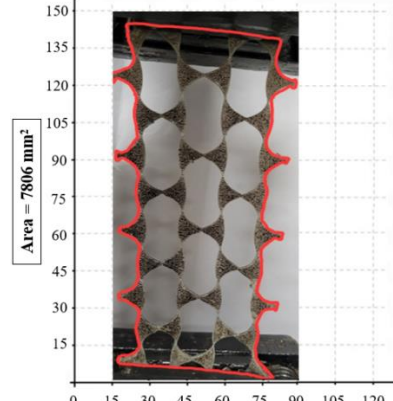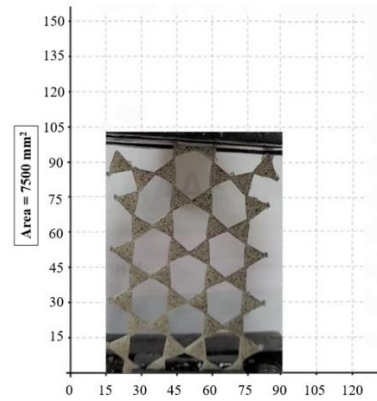
(Units of x- and y-axis in mm)

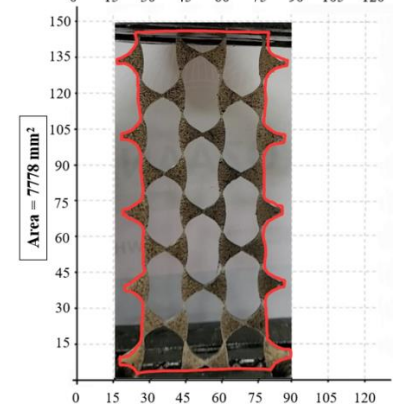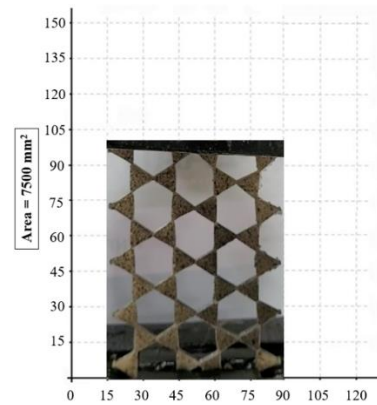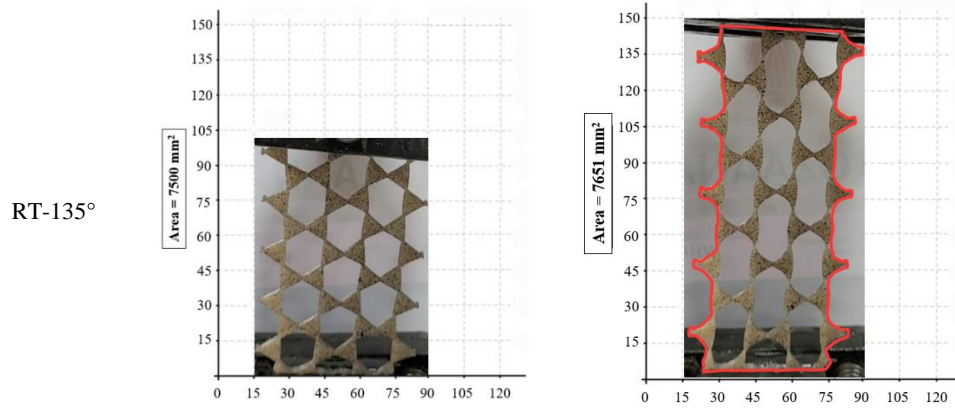| Skin Graft Simulant	Initial area	Final covered area
RT-0°		
RT-15°		
RT-30°		

RT-45°

RT-60°

RT-75°

RT-135°
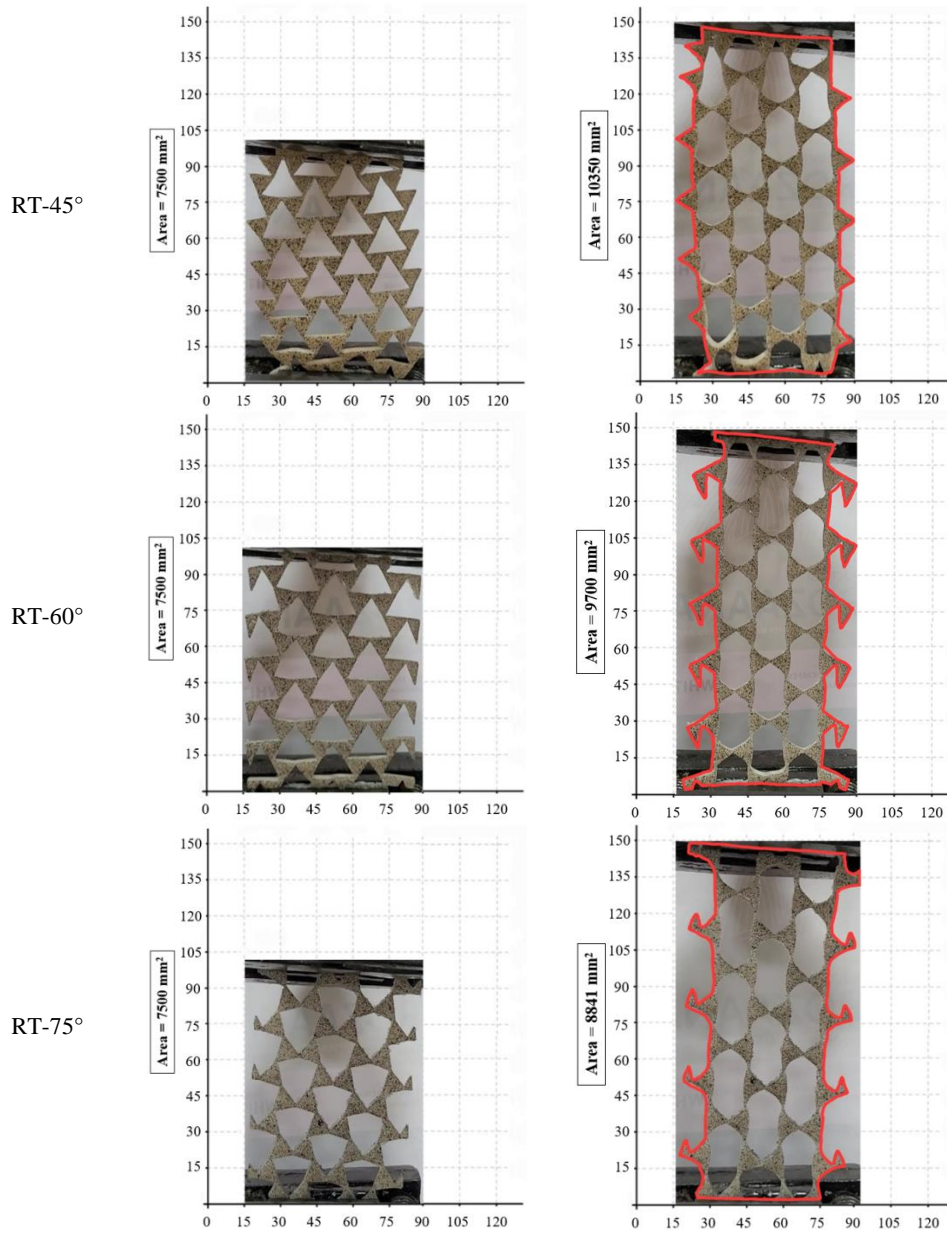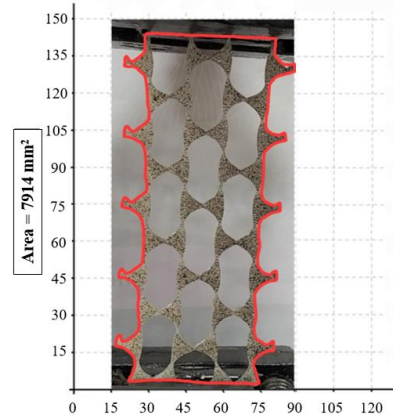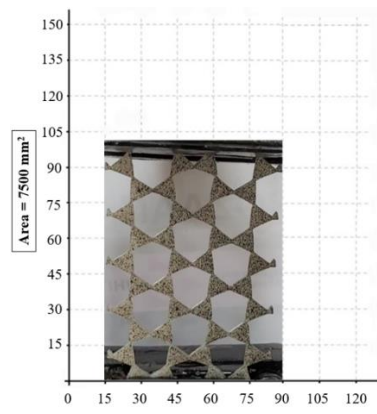
Fig. 10 presents the meshing ratios of all the graft simulants with varying RT angles, estimated at 50% strain. The meshing ratio was calculated as the ratio of the final covered area (after stretching) and the initial area (Table 1). In decreasing order, the estimated MR values were 1.76, 1.52, 1.46, 1.38, 1.29, 1.17, 1.05, 1.03, 1.02, and 1.01, for the RT-0°, RT-15°, RT-30°, RT-45°, RT-60°, RT-75°, RT-90°, RT-120°, RT-135°, and RT-105° respectively. The MRs of the RT skin graft simulants were found to be higher than the meshing ratios of traditional skin grafts. From a clinical perspective, a skin graft with a high meshing ratio exhibits potential to cover large burn areas with minimum amount of available donor skin.
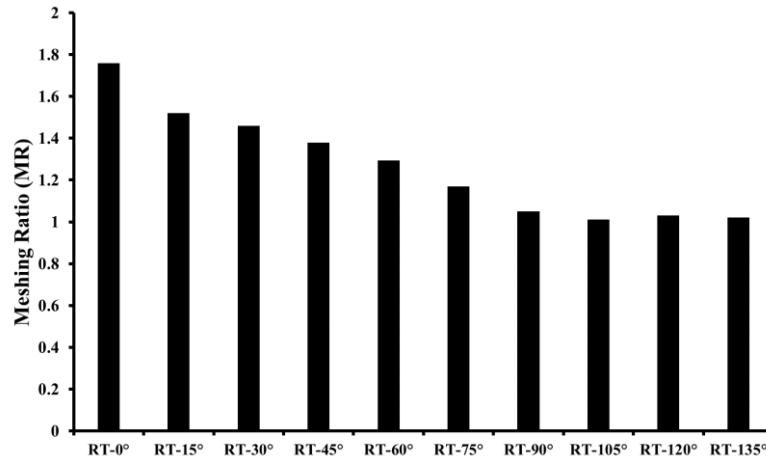

Fig. 10 Uniaxial Meshing ratios for RT skin graft simulants at 50% strain

4. CONCLUSIONS

In this work, a novel experimental framework was developed to study the expansion potential of skin grafts with rotating triangle shaped auxetic incisions. A biofidelic skin

simulant material was employed to fabricate auxetic skin graft simulants with a range of rotating triangle variants, using additive manufacturing and biomimetics. The stress-strain behavior, induced strain response, and expansions of the skin graft simulants were characterized using tensile testing and DIC analysis. With low induced stresses and high expansions, the 0° model was found to be the most suitable auxetic graft structure compared to other models. These findings are comparable with previously reported observations in rotating triangle based auxetic polymers [31-33]. The 105° model exhibited minimal expansion with high induced stresses, making it the least ideal auxetic for skin graft expansions. It was observed that only four out of ten skin graft simulants, namely the 0°, 15°, 30°, and 45° models showed auxetic and elastic expansion. Two additional simulants (i.e., 60° and 75° models) exhibited expansions beyond their size purely due to elasticity. Such findings are novel and have not been reported so far on skin graft expansions.

A few limitations of this work should be acknowledged. An isotropic biofidelic skin simulant was employed instead of actual skin to the study the effect of rotating triangle shaped auxetic incision patterns on the skin graft expansions. To maintain uniformity in the analyses, the skin graft simulant area and thickness were fixed. In reality, human skin exhibits anisotropic behavior and skin grafts vary widely in shapes and thicknesses. In future studies, cadaveric skin with varying shapes and thicknesses will be projected with the auxetic patterns through innovative meshing techniques for more accurate analyses.

In conclusion, the rotating triangle shaped auxetic incision patterns exhibited the potential for expansions higher than in traditional skin grafts. The degree of expansion was found to be tuneable without causing skin rupture through modification of the auxetic's internal angle. With further clinical trials and validations, skin grafting using the tested auxetic incisions may allow the covering of large burn areas using a small amount of donor skin.

REFERENCES

1. Gupta, V., Chanda, A., 2021, *Expansion potential of skin grafts with novel I-shaped auxetic incisions,* Biomedical Physics &Engineering Express, 8(1), 015016.
2. Henderson, J., Arya, R., Gillespie, P., 2012, *Skin graft meshing, over-meshing and cross-meshing,* International Journal of Surgery, 10(9), pp. 547–550.
3. Swaim, S.F., 1990, *Skin Grafts,* Veterinary Clinics of North America: Small Animal Practice, 20(1), pp. 147–175.
4. Kanapathy, M., Hachach-Haram, N., Bystrzonowski, N., 2016, *Epidermal grafting versus split-thickness skin grafting for wound healing (EPIGRAAFT): study protocol for a randomized controlled trial,* Trials, 17, 245.
5. Asuku, M., Yu, T.C., Yan, Q., Boing, E., Hahn, H., 2001, *Split-thickness skin graft donor-site morbidity: a systematic literature review,* Burns, 47(7), pp. 1525–1546.
6. Serebrakian, A.T., Pickrell, B.B., Varon, D.E., Mohamandi, A.M.D., Grinstaff, M.W., 2018, *Meta-analysis and systematic review of skin graft donor-site dressings with future guidelines,* Plastic and Reconstructive Surgery-Global Open, 6(9), e1928.
7. Vandeput, J., Nelissen, M., Tanner, J.C., Boswick, J., 1995, *A review of skin meshers,* Burns, 21(5), pp. 364–370.

8. Lyons, J.L., Kagan, R.J., 2014, *The true Meshing Ratio of Skin Graft Meshers,* Journal of Burn Care& Research, 35(3), pp. 257–260.

9. Grima, J.N., Gatt, R., 2010, *Perforated sheets exhibiting negative Poisson's ratios,* Advanced Engineering Materials, 12(6), pp. 460–464.

10. Dudek, K.K., Gatt, R., Mizzi, L., Dudek, M.R., Attard, D., Evans, K.E.,Grima, J.N.,2017, *On the dynamics and control of mechanical properties of hierarchical rotating rigid unit auxetics,* Scientific Reports, 7(1), pp. 1–9.

11. Singh, G., Chanda, A., 2021, *Mechanical properties of whole-body soft human tissues: a review,* Biomedical Materials,16(6), 062004.

12. Nosrati, H., Khodaei, M., Alizadeh, Z., Banitalebi-Dehkordi, M., 2021, *Cationic, anionic and neutral polysaccharides for skin tissue engineering and wound healing applications,* International Journal of Biological Macromolecules, 192, pp. 298–322.

13. Geerligs, M., van-Breemen, L., Peters, G., Ackermans, P., Baaijens, F., Oomens, C., 2011, *In vitro indentation to determine the mechanical properties of epidermis,* Journal of Biomechanics, 44(6), pp. 1176–1181.

14. Yuan, J., Dagdeviren, C., Shi, Y., Ma, Y., Feng, X., Rogers, J.A., Huang, Y., 2016, *Computational models for the determination of depth-dependent mechanical properties of skin with a soft, flexible measurement device,* Proceedings of the Royal Society A: Mathematical, Physical and Engineering Sciences, 472(2194), pp. 1–17.

15. Makode, S., Singh, G., Chanda, A., 2021, *Development of novel anisotropic skin simulants,* Physica Scripta, 96(12), 125019.

16. Gupta, V., Chanda, A., 2022, *Biomechanics of skin grafts: effect of pattern size, spacing and orientation,* Engineering Research Express, doi: 10.1088/2631-8695/AC48CB.

17. Mizzi, L., Grima, J.N., Gatt, R., Attard, D., 2019, *Analysis of the deformation behavior and mechanical properties of slit-perforated auxetic metamaterials,* Physica Status Solidi (B), 256(1), 1800153.

18. Chanda, A., Unnikrishnan, V., Lackey, K., Robbins, J., 2019, *Biofidelic conductive soft tissue surrogates,* International Journal of Polymeric Materials and Polymeric Biomaterials, 69(2), pp. 127–135.

19. Chanda, A., 2018, *Biomechanical modeling of human skin tissue surrogates,* Biomimetics, 3(3), 18.

20. Ni-Annaidh., A., Bruyere, K., Destrade, M., Gilchrist, M.D., Ottenio, M., 2012, *Characterization of the anisotropic mechanical properties of excised human skin,* Journal of Mechanical Behavior of Biomedical Materials, 5(1), pp. 139–148.

21. Witte, M., Rübhausen, M., Jaspers, S., Wenck, H., Fischer, F., 2021, *A method to analyze the influence of mechanical strain on dermal collagen morphologies,* Scientific Reports, 11(1), pp. 1–8.

22. Shergold, O.A., Fleck, N.A., Radford, D., 2006, *The uniaxial stress versus strain response of pig skin and silicone rubber at low and high strain rates,* International Journal of Impact Engineering, 32(9), pp. 1384–1402.

23. Gupta, V., Singh, G., Chanda, A., 2022, *Development and testing of skin grafts models with varying slit orientations,* Materials Today: Proceedings, 62(6), pp. 3462-3467.

24. Singh, G., Gupta, V., Chanda, A., 2022, *Artificial skin with varying biomechanical properties,* Materials Today: Proceedings, 62(6), pp. 3162-3166.

25. Chanda, A., Weston, A., 2018, *Biomechanical modeling of wounded skin,* Journal of Composites Science, 2(4), 69.

26. Blumenfeld, R., Edwards, S.F., 2012, *Theory of strains in auxetic materials,* Journal of Superconductivity and Novel Magnetism, 25(3), pp. 565–571.

27. Gaspar, N., Ren, X.J., Smith, C.W., Grima, J.N., Evans, KE., 2005, *Novel honeycombs with auxetic behaviour*, ActaMaterialia, 53(8), pp. 2439–2445.

28. Grima, J.N., Chetcuti, E., Manicaro, E., Attard, D., Camilleri, M., Gatt, R., Evans, K.E., 2012, *On the auxetic properties of generic rotating rigid triangles,*Proceedings of the Royal Society A: Mathematical, Physical and Engineering Sciences, 468(2139), pp. 810–830.

29. Dubrovski, P.D., Novak, N., Borovinsek, M., Vesenjak, M., Ren, Z., 2019, *In-plane behavior of auxetic non-woven fabric based on rotating square unit geometry under tensile load,* Polymers, 11(6), 1040.

30. Gao, Y.K., 2021, *Auxetic metamaterials and structures,* Journal of Materials Engineering, 49(5), pp. 38–47.

31. Evans, K.E., 1991, *Auxetic polymers: a new range of materials,* Endeavour, 15(4), pp.170–174.

32. Greaves, G.N., Greer, A.L., Lakes, R.S., Rouxel, T., 2011, *Poisson's ratio and modern materials,* Nature Materials, 10(11), pp. 823–837.

33. Mir, M., Ali, M.N., Sami, J., Ansari, U., 2014, *Review of mechanics and applications of auxetic structures,* Advances in Materials Science and Engineering, 2014, 753496.